An Ab Initio Study of the Structures and Vibrational Spectra of Chromium Oxo-Anions and Oxyhalides

Stephen Bell and Trevor J. Dines*

Department of Chemistry, University of Dundee, Dundee DD1 4HN, United Kingdom

Received: June 27, 2000; In Final Form: September 26, 2000

The bond distance and vibrational spectrum of the chromate(VI) ion has been calculated using HF-SCF and SCF-density functional (SCF-DFT) methods in conjunction with a wide range of basis sets. It was found that the B3-LYP/LanL2DZ combination gave the best fit for the observed vibrational spectrum. The molecular geometries and vibrational spectra of chromate(V), dichromate, trichromate, chlorochromate, fluorochromate, chromyl chloride, and chromyl fluoride were also calculated using B3-LYP/LanL2DZ. Force constants and potential energy distributions were determined from the calculated spectra, after appropriate scaling, which compare favorably with the experimental IR and Raman spectra. Precise vibrational band assignments have been determined for dichromate and trichromate. Relationships have been established between the CrO bond distance and CrO principal stretching force constant.

Introduction

In the last 20 years, there has developed considerable interest in the ab initio calculation of vibrational wavenumbers and IR and Raman intensities.[1−4] Ab initio calculations provide a complete set of force constants, from which a potential energy distribution may be determined for every normal coordinate. However, calculations at the Hartree−Fock (HF-SCF) level yield force constants that are consistently high for three reasons: (i) such calculations tend to give excessively short bond lengths, even shorter with large basis sets; (ii) electron correlation is neglected, leading to a poor estimate of the electron density between atoms; and (iii) the harmonic oscillator approximation is assumed. The latter, in particular, leads to abnormally high wavenumbers for vibrations that are known to be appreciably anharmonic, e.g., for the stretching of bonds involving hydrogen atoms. Typically, force constants computed at the HF-SCF level require scaling by factors of the order of 0.80−0.85 and are not generally improved by invoking larger basis sets than 3-21G. More realistic calculations of both molecular geometries and force fields require calculation at the MP2 level with at least a 6-31+G(d) basis set, which generally yields vibrational wavenumbers that are within 2−3% of the experimental values, whence most of the deviation is accounted for by anharmonicity and possibly also Fermi resonance.

In the past few years, hybrid SCF-density functional methods (SCF-DFT),[5] particularly B3-LYP (which incorporates Becke's three parameter Hybrid Functional[6] and the Lee, Yang and Parr correlation functional),[7] have become popular[8−10] since they provide vibrational wavenumbers that are comparable with or better than those obtained at the MP2 level but require significantly less computation time. For molecules involving transition metals only small basis sets can be used for the transition metal atoms because of limits on computer resources. For small molecules containing lighter atoms, when large bases can be employed with the B3-LYP method, excellent agreement is obtained with experimental bond lengths.[11] It has been noted[12] for a number of compounds with C═O and C≡C bonds that SCF-DFT calculations yield bond lengths much nearer to experimental data than those obtained by HF-SCF calculations, which are very short, or MP2 methods, which are very long. The calculation of vibrational spectra of molecules containing transition metals becomes prohibitively expensive at the MP2 level and lower levels of theory must suffice. Furthermore, the range of basis sets available for transition metals is restricted.

In this paper, we report the results of SCF-DFT studies of the molecular geometries and vibrational spectra of several chromium oxo-anions and oxyhalides. The vibrational spectroscopic characterization of chromium oxo species is of particular relevance to the interpretation of the IR and Raman spectra of supported chromium oxide catalysts. Chromium(VI) oxide species supported on oxides such as silica, alumina, or titania are used as oxidation catalysts and silica-supported chromium(VI) oxide is the precursor to the Philips catalyst for alkene polymerization, in which chromium is in a lower oxidation state. It has been shown, principally by Raman and UV−visible diffuse reflectance spectroscopy that the nature of the chromium oxo species is dependent on conditions of catalyst preparation, specifically the chromium loading, the support oxide, and the state of hydration.[13−22] Accordingly, the surface chromium species may be a monochromate with attachment to the support through two or three oxygen atoms, a polychromate species, or at high chromium loading may be found as bulk CrO_3. To derive detailed structural information from these systems, we have carried out Raman and ab initio studies, which will be reported in a future paper. The interpretation of these results has necessitated a survey of the vibrational spectra of a wide range of model chromium oxo species, including normal coordinate analyses and calculation of force constants.

Theoretical Procedures

Ab initio calculations were performed using the Gaussian 98 program,[23] initially at the HF-SCF level with the 3-21+G basis set. Subsequently, HF-SCF and SCF-DFT calculations were

* To whom correspondence should be addressed. E-mail: t.j.dines@dundee.ac.uk; fax: 44-1382-345517.

10.1021/jp002312u CCC: $19.00
Published on Web 11/10/2000

carried out using larger basis sets. These included the split-valence basis sets 6-31G and 6-311G and some double-ζ (DZ) basis sets. The most satisfactory results were obtained using the LanL2DZ basis set, which employs Dunning−Huzinaga DZ basis functions on the first row elements and Los Alamos effective core potential with DZ functions on heavier atoms.[24] After satisfactory geometry optimization the vibrational spectrum of each species was calculated. For computation of the potential energy distributions associated with the vibrational modes, the Cartesian force constants obtained from the Gaussian 98 output were converted to force constants expressed in terms of internal coordinates and scaled before input to a normal coordinate analysis program derived from those of Schachtschneider.[25] In each case, the calculated geometries and vibrational spectra were compared with the most recent experimental data available in the literature.

Results and Discussion

$[CrO_4]^{2-}$ and $[CrO_4]^{3-}$. The molecular geometry and vibrational spectrum of $[CrO_4]^{2-}$ was calculated using the HF-SCF, MP2, and several different SCF-DFT methods with a variety of basis sets to ascertain the most suitable combination of method and basis set. It was found that MP2 calculations yielded excessively large bond distances, typically around 1.75 Å, and low vibrational wavenumbers; these results are therefore not presented. The results of the HF-SCF and SCF-DFT calculations are surveyed in Tables 1 and 2 and Figures 1−3. It is clear that calculations at the HF level yield an over short Cr−O bond length, with respect to the value of 1.647 Å determined crystallographically for $CaCrO_4$ by Weber and Range,[26] although in some instances, with extended basis sets, the geometry failed to optimize. The $CaCrO_4$ crystal structure was chosen in preference to those of other chromate salts because the chromate ion has tetrahedral site symmetry. HF-SCF calculations of the vibrational spectrum give excessively high band wavenumbers, which become significantly worse for larger basis sets, and these results are not presented. Table 1 lists the bond distances calculated at the HF-SCF and B3-LYP levels as a function of basis set, and Figures 1−3 presents the calculated (B3-LYP) vibrational spectra for the basis sets LanL2DZ, 6-31G, and 6-311G, with additional diffuse and polarization functions. In Table 2 are listed the bond distance and vibrational band wavenumbers calculated with different SCF-DFT methods in conjunction with the LanL2DZ basis set. By far the best results, in terms of both geometry and vibrational spectrum, were achieved by the B3-LYP/LanL2DZ calculation. Even with no scaling and no additional basis functions, the calculated vibrational wavenumbers are within ca. 2% of the experimental ones, with the single exception of the ν_2(e) vibration, and the CrO bond distance is only 1.2% larger than that obtained from crystallographic data. The bond distance is improved by addition of further basis functions, but this leads to no further improvement in the molecular vibrations. Strictly, the calculated spectra should be compared with harmonic band wavenumbers, although for $[CrO_4]^{2-}$ the only harmonic data is for $\nu_1(a_1)$ for which the values $\omega_1 = 854.4$ and $x_{11} = 0.71$ cm^{-1} have been determined from a measurement of the $\nu_1\nu_1$ progression in the resonance Raman spectrum of solid $K_2[CrO_4]$.[27] Thus the anharmonicity is very small for the totally symmetric stretch, and it may reasonably be assumed that this is the case for the other vibrations. However, the larger discrepancy between the experimental and calculated wavenumber for ν_2(e) may be evidence that this mode has a larger degree of anharmonicity.

Calculations involving the larger 6-31G and 6-311G basis sets generally gave a good fit to the bond distance, especially after incorporation of diffuse and polarization functions, but proved to be a poor model for the vibrational spectra. In particular, the symmetric and antisymmetric stretching vibrations were generally much too high and in some instances close together. The plots in Figures 2 and 3 show a sawtooth pattern in which the peaks result from calculations involving only polarization functions and the troughs from calculations involving diffuse and polarization functions. It is clear from these results that extended basis sets are not necessarily beneficial in terms of vibrational spectra calculations and add a very significant computational cost. It is generally recognized that split-valence basis sets such as 6-31G and 6-311G are less satisfactory than double-ζ basis sets. However the Dunning−Huzinaga double-ζ basis set is not provided for transition metals, and it is therefore necessary to use the LanL2DZ set which uses an effective core potential for the inner chromium electrons. Table 2 lists the results of the B3-LYP/LanL2DZ calculation, together with results obtained with other hybrid SCF-DFT methods, and two recently reported DFT calculations. The other

TABLE 1: Effect of Method and Basis Set on the Calculated Bond Distance (Å) for $[CrO_4]^{2-}$

basis set	no. of basis functions	HF	B3-LYP
LanL2MB	33	1.600	1.672
STO-3G	43	1.505	1.542
3-21G	65	1.604	
3-21+G	81	1.623	1.669
SDD	89	1.613	1.662
CEP-4G	50	1.626	1.676
CEP-31G	66	1.628	1.677
CEP-121G	82	1.628	1.677
SV	57	1.607	1.650
SVP	80	1.597	1.645
Ahlrichs VDZ	57	1.607	1.650
Ahlrichs pVDZ	80	1.597	1.645
Ahlrichs VTZ	86	1.623	1.675
LanL2DZ	58	1.620	1.667
LanL2DZ with diffuse *p* on O	70	1.619	1.667
LanL2DZ with *d* on O	78	1.605	1.655
LanL2DZ with *d* and diffuse *p* on O	90	1.604	1.655
LanL2DZ with *d* and diffuse *p* on O and *f* on Cr	97	1.597	1.649
6-31G	65	1.624	1.669
6-31G(d)	96	1.597	1.648
6-31G(2d)	127	1.600	1.651
6-31G(3d)	158	1.597	1.648
6-31G(df)	133	1.594	1.645
6-31G(2df)	164	1.597	1.647
6-31G(3df)	195	1.595	1.645
6-31+G	94	1.630	1.678
6-31+G(d)	125	1.606	1.657
6-31+G(2d)	156		1.657
6-31+G(3d)	187		1.656
6-31+G(df)	162	1.604	1.655
6-31+G(2df)	193	1.603	1.655
6-31+G(3df)	224	1.602	1.654
6-311G	91	1.618	1.667
6-311G(d)	118	1.596	1.648
6-311G(2d)	145	1.601	1.651
6-311G(3d)	172	1.600	
6-311G(df)	155	1.595	1.647
6-311G(2df)	182	1.599	1.648
6-311G(3df)	209	1.599	1.648
6-311+G	119	1.626	1.679
6-311+G(d)	146	1.602	1.658
6-311+G(2d)	173	1.606	1.659
6-311+G(3d)	200	1.750	1.659
6-311+G(df)	183		1.656
6-311+G(2df)	210		1.658
6-311+G(3df)	237		1.658

TABLE 2: Comparison of Molecular Geometry and Vibrational Wavenumbers for $[CrO_4]^{2-}$ Calculated by Hybrid SCF-DFT Methods with the LanL2DZ Basis Set

		wavenumber /cm^{-1}			
method	r(CrO) (Å)	$\nu_1(a_1)$	$\nu_2(e)$	$\nu_3(t_2)$	$\nu_4(t_2)$
B3-LYP	1.667	853	333	906	377
B1-LYP	1.664	863	336	912	381
B3-P86	1.658	873	338	929	382
B3-PW91	1.660	866	337	921	381
MPW1-PW91	1.654	882	341	934	385
BHandH	1.624	961	362	1002	408
BHandH-LYP	1.638	927	357	961	404
LDA/DZP[a]	1.658	836	332	894	356
LDA/TZP[a]	1.658	866	323	912	356
GC/TZP[a]	1.658	870	330	926	380
LDA/TZP[b]	1.661	857	330	904	369
expt[c]	1.647	846	349	890	378

[a] Deeth and Sheen (ref 28), local density approximation (LDA), or nonlocal gradient approximation (GC) and double-ζ or triple-ζ basis set with polarization functions. [b] Stückl et al. (ref 29) local density approximation (LDA) and triple-ζ basis set with polarization functions. [c] Bond distance (ref 26, Ca^{2+} salt), vibrational spectrum (ref 27, solution, K^+ salt).

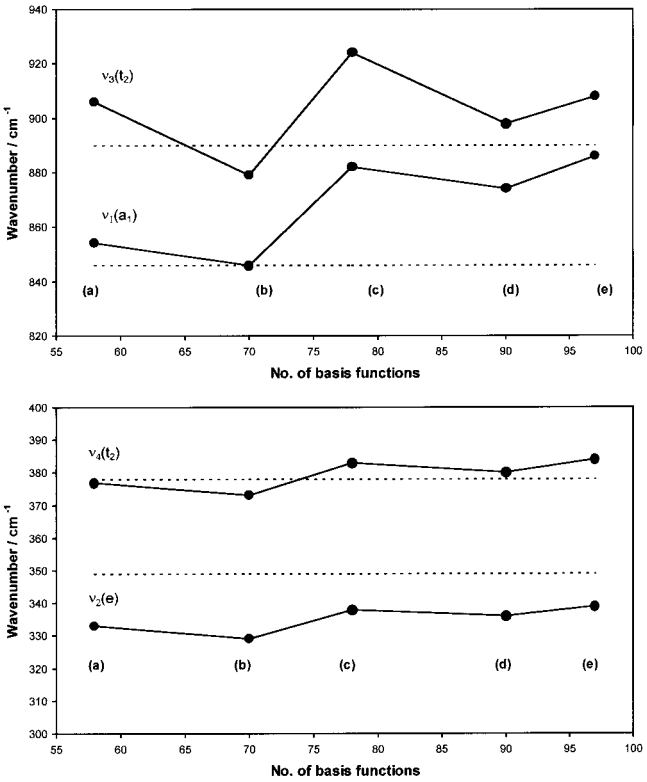

Figure 1. Variation of vibrational band wavenumbers of $[CrO_4]^{2-}$ for B3-LYP calculations with the LanL2DZ basis set (a) and the following additional functions: (b) diffuse *p* functions on oxygen atoms, (c) polarization *d* functions on oxygen atoms, (d) diffuse *p* and polarization *d* functions on oxygen atoms, and (e) diffuse *p* and polarization *d* functions on oxygen atoms and polarization *f* functions on the chromium atom.

methods gave less satisfactory results than the B3-LYP method which has proved to be the most popular for modeling vibrational spectra.

The calculated force constants for $[CrO_4]^{2-}$ were scaled, and these are listed together with the scaled vibrational wavenumbers in Table 3. Because of the superiority of the B3-LYP/LanL2DZ calculation for $[CrO_4]^{2-}$, this method was also used for the other chromate species, and in each case significantly better results were obtained than with other basis sets. There have been several

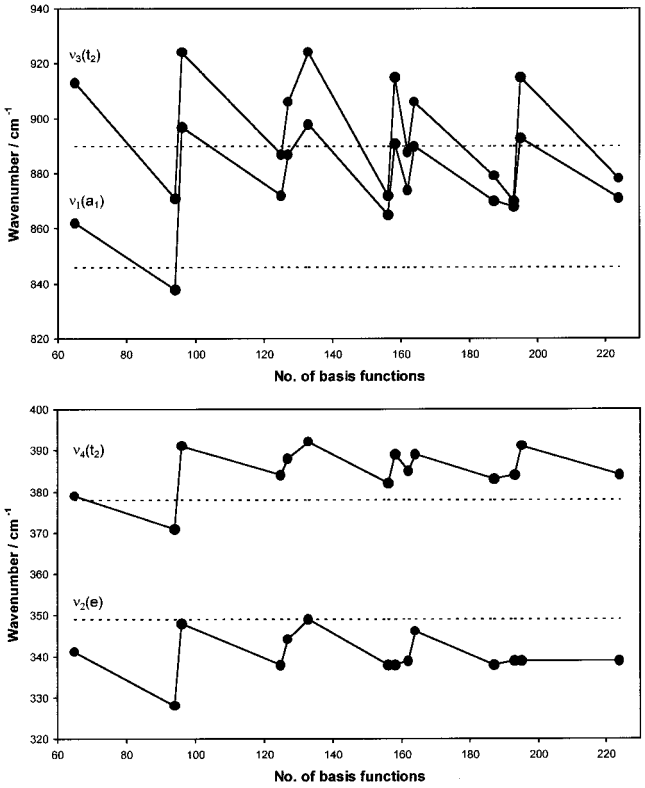

Figure 2. Variation of vibrational band wavenumbers of $[CrO_4]^{2-}$ for B3-LYP calculations with the 6-31G basis set and additional diffuse and polarization functions.

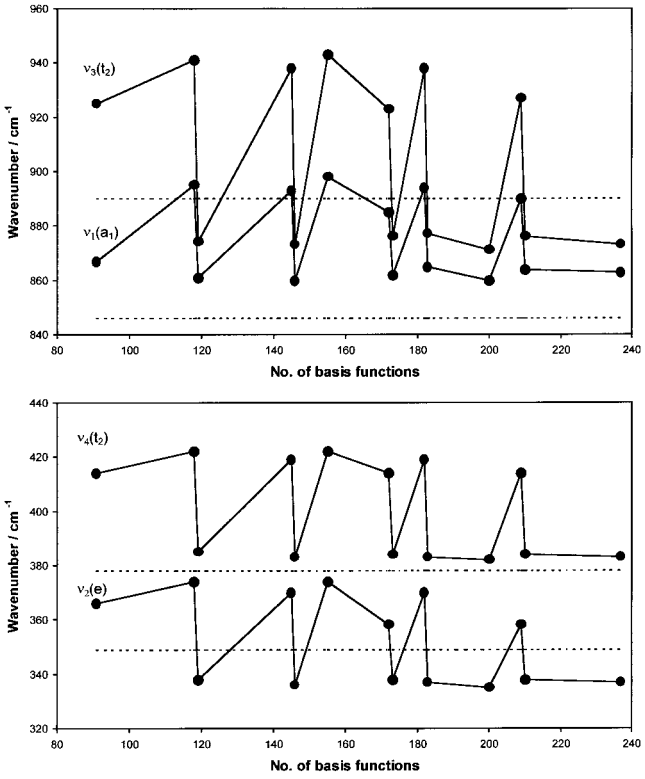

Figure 3. Variation of vibrational band wavenumbers of $[CrO_4]^{2-}$ for B3-LYP calculations with the 6-311G basis set and additional diffuse and polarization functions.

measurements of the IR and Raman spectra of chromate(VI) salts in the solid state and in solution, although the most recent data, reported by Weinstock et al.,[30] is considered the most reliable. After scaling of the force constants, the calculated band

TABLE 3: Comparison of Scaled B3-LYP/LanL2DZ Vibrational Wavenumbers with the Experimental Data, and Calculated Force Constants (mdyn Å^{-1}) for $[CrO_4]^{2-}$

Vibrational Wavenumbers

	wavenumber (cm^{-1})		
	calc		
vibration	unscaled	scaled	expt[26]
$\nu_1(a_1)$	853	845	846
$\nu_2(e)$	333	336	349
$\nu_3(t_2)$	906	898	890
$\nu_4(t_2)$	377	381	378

Scaled Force Constants (mdyn Å^{-1})[a]

	calc	expt[30,32]
f[CrO]	5.530	5.48
f[CrO,CrO]	0.400	0.43
f[CrO,OCrO]	−0.026	
f[CrO,OCrO′][b]	0.026	
f[OCrO]	0.960	1.15[c]
f[OCrO,OCrO]	−0.165	0.055[c]
f[OCrO,OCrO′][b]	−0.301	

[a] Scaling factors 0.98 (CrO) and 1.02 (OCrO) for force constants. [b] The prime (′) refers to pairs of internal coordinates with no common bond. [c] The reported force constants were multiplied by r^2 to be consistent with the calculated force constants.

wavenumbers yield an excellent fit to the experimental data. The calculation enabled determination of the complete set of GVFF force constants. Force constants were calculated from the Raman spectrum by Bassi and Sala[31] and further refined by Gonzalez-Vilchez and Griffith[32] using Raman data from ^{18}O isotopomers. Nevertheless, only a limited range of force constants could be obtained from the spectroscopic data, and many of these were reported as symmetrized combinations of GVFF force constants. For this reason, only the principal and interaction stretching force constants have been included in Table 3, which are in close agreement with the calculated values after scaling of the latter.

The chromate(V) ion $[CrO_4]^{3-}$ has a d^1 configuration, in which the ^2E ground state is subject to Jahn−Teller distortion. Initial geometry optimization was carried out with T_d symmetry, but a significantly lower energy structure was obtained on allowing a distortion to D_{2d} symmetry, corresponding to Jahn−Teller distortion along the $Q_2(e)$ normal coordinate. The calculated bond distances and interbond angles, vibrational wavenumbers, and force constants are listed in Table 4, together with the experimental data. The only structural data reported for chromate(V) is for $Ca_5[CrO_4]OH$,[33] from which the bond distance is close to the calculated value but only marginally larger than that of chromate(VI). This is a little surprising in that the additional electron, with respect to chromate(VI), is in an antibonding (e) orbital, in which case a significantly longer bond distance would have been anticipated.

Vibrational data for chromate(V) is somewhat sparse, and the only complete set of IR and Raman band positions is that reported by Gonzalez-Vilchez and Griffith.[32] Their solution Raman data are consistent with tetrahedral geometry, indicating that the Jahn−Teller effect is dynamic, and no permanent distortion occurs at room temperature. Although the calculated band positions, after scaling, agree well for three of the vibrations, we were unable to obtain a satisfactory fit to $\nu_2(e)$, which therefore brings into question the assignment of this vibration to the band reported at 260 cm^{-1}. In the same paper, Gonzalez-Vilchez and Griffith also report vibrational data for several other transition metal tetraoxo-anions, and inspection

TABLE 4: Calculated (B3-LYP/LanL2DZ) Molecular Geometry, Vibrational Wavenumbers, and Force Constants for $[CrO_4]^{3-}$

Molecular Geometry

	calc	expt[33]
r(Cr═O) (Å)	1.668	1.66
θ(OCrO) (deg)	110.0	
θ(OCrO′) (deg)	109.2	

Vibrational Wavenumbers

vibration		wavenumber (cm^{-1}) calc.		
T_d	D_{2d}	unscaled	scaled	expt[32]
$\nu_1(a_1)$	a_1	852	830	834
$\nu_2(e)$	b_1	335	299	260
	a_1	330	295	
$\nu_3(t_2)$	b_2	894	868	860
	e	890	863	
$\nu_4(t_2)$	b_2	368	330	324
	e	354	318	

Scaled Force Constants (mdyn Å^{-1})[a]

f[CrO]	5.172
f[CrO,CrO]	0.410, 0.504
f[CrO,OCrO]	−0.031, −0.069
f[CrO,OCrO′][b]	0.072, 0.025
f[OCrO]	0.725, 0.709
f[OCrO,OCrO]	−0.127, −0.132
f[OCrO,OCrO′][b]	−0.192, −0.214

[a] Scaling factors 0.95 (CrO) and 0.80 (OCrO) for force constants. [b] The prime (′) refers to pairs of internal coordinates with no common bond.

of their data reveals that the assignment of $\nu_2(e)$ for chromate(V) does not fit into the general pattern. We therefore suggest that the 260 cm^{-1} band is an experimental artifact and that the true position of $\nu_2(e)$ is close to the calculated value (295, 299 cm^{-1}), in which case it may be overlapped by $\nu_4(t_2)$.

$[CrO_3X]^-$ and CrO_2X_2 (X = F, Cl). The results of B3-LYP/LanL2DZ calculations on the halochromate ions and the chromyl halides are listed in Tables 5 and 6, respectively. The calculated CrO bond distances for the $[CrO_3X]^-$ anions are comparable with those determined from crystallographic measurements, but the CrX distances are significantly different. The molecular geometries of the CrO_2X_2 species were obtained from electron diffraction measurements,[38,39] and the calculated bond distances and bond angles compare favorably with the experimental data. GVFF force constants were determined from the electron diffraction measurements, in conjunction with spectroscopic data, but these were presented in the symmetry-adapted form. However, they compare favorably with symmetry-adapted force constants from our scaled B3-LYP/LanL2DZ GVFF force constants. There are some discrepancies that can be attributed to the fact that, for the experimentally determined force field, many interaction force constants were necessarily set equal to zero. For both molecules, the scaled vibrational spectrum gave a good fit to the experimental data[40,41] although it was found that the calculated wavenumbers for the symmetric and antisymmetric CrO stretches were much closer together than is observed.

$[Cr_2O_7]^{2-}$ and $[Cr_3O_{10}]^{2-}$. The results of B3-LYP/LanL2DZ calculations on $[Cr_2O_7]^{2-}$ and $[Cr_3O_{10}]^{2-}$ are listed in Tables 7 and 8, respectively. For both of these species, full geometry optimization resulted in near-linear geometry at the bridging oxygen atoms. This was also found to be the case with other basis sets and when using the HF method, even with inclusion of diffuse functions and polarization functions (d orbitals on

TABLE 5: Calculated (B3-LYP/LanL2DZ) and Experimental Molecular Geometry and Vibrational Wavenumbers (cm^{-1}) for $[CrO_3X]^-$ (X = F, Cl) and Force Constants (mdyn $Å^{-1}$)

Molecular Geometry

	$[CrO_3F]^-$			$[CrO_3Cl]^-$		
	calc	expt[34]	scale factor	calc	expt[35]	scale factor
r(CrO) (Å)	1.614	1.633	0.875	1.610	1.533	0.91
r(CrX) (Å)	1.792	1.633	0.905	2.276	2.162	1.25
θ(OCrO) (deg)	110.7	109.5	0.94	111.1	106.2	0.90
θ(OCrX) (deg)	108.2	109.5	0.97	107.8	111.8	1.15

Vibrational Wavenumbers

		$[CrO_3F]^-$			$[CrO_3Cl]^-$		
		calc			calc		
		unscaled	scaled	expt[36]	unscaled	scaled	expt[37]
$\nu_1(a_1)$	ν(CrO)	970	908	911	973	928	935
$\nu_2(a_1)$	ν(CrX)	669	637	637	410	438	438
$\nu_3(a_1)$	δ(OCrO)	349	340	338	288	304	295
ν_4(e)	ν(CrO)	1030	964	955	1035	987	954
ν_5(e)	δ(OCrO)	369	370	370	358	365	365
ν_6(e)	δ(OCrX)	264	261	261	209	209	209

Force Constants

	$[CrO_3F]^-$		$[CrO_3Cl]^-$	
	calc	expt[36]	calc	expt[37]
f[CrO]	6.345	6.26	6.684	6.29
f[CrX]	3.290	3.36	2.059	2.00
f[CrO,CrO]	0.378	0.28	0.395	0.31
f[CrO,CrX]	0.175		0.116	
f[CrO,OCrO]	−0.010		−0.012	
f[CrX,OCrO]	−0.019		−0.046	
f[CrO,OCrO′]	0.061		0.059	
f[CrO,OCrX]	0.005		0.010	
f[CrX,OCrX]	0.021		0.049	
f[CrO,OCrX′][a]	−0.052		−0.057	
f[OCrO]	0.871	0.44	0.819	0.43
f[OCrX]	0.631	0.23	0.610	0.17
f[OCrO,OCrO]	−0.200	0.02	−0.180	0.02
f[OCrX,OCrX]	−0.057		−0.041	
f[OCrO,OCrX]	−0.137		−0.142	
f[OCrO,OCrX′]	−0.218		−0.207	

[a] The prime (′) refer to pairs of internal coordinates with no common bond.

oxygen and f orbitals on chromium). For this reason, geometry optimization of $[Cr_2O_7]^{2-}$ was repeated with the CrOCr bond angle constrained to the experimentally determined value of 123.9°,[42] although this yielded one imaginary vibrational wavenumber, corresponding to a CrO torsional mode. The near-linear CrOCr angle predicted by both HF and B3-LYP calculations suggests that there is a significant π contribution to the bridging CrO bonds. This is not supported by experimental evidence since both the structure in the solid state, from X-ray diffraction measurements, and the IR and Raman spectra in solid and solution are consistent with a nonlinear C_{2v} geometry. Nevertheless, the energy differences between the constrained and the fully optimized geometries was only 23.04 kJ mol^{-1}. It may be the case that a near-linear structure is the optimum geometry for isolated $[Cr_2O_7]^{2-}$ in the gas phase but that crystal packing forces in the solid state, or hydrogen bonding in aqueous solution, favor the nonlinear geometry. We performed an additional set of calculations in which $[Cr_2O_7]^{2-}$ was hydrogen-bonded to eight water molecules and the SCRF Onsager solvation model was employed,[43] with solute radius 5.22 Å and dielectric constant 78.39. This resulted in a fully optimized geometry with the CrOCr angle at 133.8°. All force constants relating to motions of the hydrogen-bonded water molecules were removed prior to calculation of the vibrational wavenumbers and potential energy distributions, which are listed in Table

TABLE 6: Calculated (B3-LYP/LanL2DZ) and Experimental Molecular Geometry and Vibrational Wavenumbers (cm^{-1}) for CrO_2X_2 (X = F, Cl) and Force Constants (mdyn $Å^{-1}$)

Molecular Geometry

	CrO_2F_2			CrO_2Cl_2		
	calc	expt[38]	scale factor	calc	expt[39]	scale factor
r(CrO) (Å)	1.570	1.572	0.87	1.569	1.577	0.845
r(CrX) (Å)	1.725	1.716	0.915	2.157	2.122	1.18
θ(OCrO) (deg)	108.3	107.8	0.97	109.1	108.5	0.86
θ(OCrX) (deg)	110.7	109.3	1.06	109.2	108.7	0.98
θ(XCrX) (deg)	109.5	111.9	1.17	111.1	113.2	1.10

Vibrational Wavenumbers

		CrO_2F_2			CrO_2Cl_2		
		calc			calc		
		unscaled	scaled	expt[40]	unscaled	scaled	expt[41]
$\nu_1(a_1)$	ν(CrO)	1087	1015	995	1076	990	991
$\nu_2(a_1)$	ν(CrX)	741	710	708	432	464	470
$\nu_3(a_1)$	δ(OCrO)	412	408	403	358	356	356
$\nu_4(a_1)$	δ(XCrX)	206	220	220	134	139	139
$\nu_5(a_2)$	τ	281	275	275	220	219	224
$\nu_6(b_1)$	ν(CrX)	802	769	770	473	510	503
$\nu_7(b_1)$	δ(OCrO)	311	320	325	268	268	257
$\nu_8(b_2)$	ν(CrO)	1106	1033	1045	1093	1005	1002
$\nu_9(b_2)$	δ(XCrX)	288	296	295	214	212	212

Scaled GVFF Force Constants[a]

	CrO_2F_2	CrO_2Cl_2		CrO_2F_2	CrO_2Cl_2
f[CrO]	7.443	7.122	f[CrX,OCrX′]	−0.035	−0.071
f[CrX]	4.491	2.857	f[CrX,XCrX]	−0.050	−0.004
f[CrO,CrO]	0.427	0.442	f[OCrO]	1.110	0.938
f[CrX,CrX]	0.116	0.052	f[XCrX]	0.460	0.458
f[CrO,CrX]	0.196	0.129	f[OCrO,OCrX]	−0.209	−0.175
f[CrO,OCrO]	0.013	−0.008	f[OCrO,XCrX]	−0.246	−0.214
f[CrO,XCrX]	−0.010	−0.002	f[XCrX,OCrX]	−0.057	−0.064
f[CrO,OCrX]	−0.018	−0.008	f[OCrX]	0.656	0.553
f[CrO,OCrX′]	0.017	0.014	f[OCrX,OCrX]	−0.116	−0.081
f[CrX,OCrO]	0.027	−0.027	f[OCrX,OCrX′]	−0.166	−0.141
f[CrX,OCrX]	0.047	0.086	f[OCrX,OCrXO]	−0.112	−0.096

Symmetry-Adapted Scaled Force Constants[b]

			CrO_2F_2		CrO_2Cl_2	
			calc	exp[38]	calc	exp[39]
A_1	F_{11}	F[CrO]	7.870	7.811	7.565	7.656
	F_{22}	F[CrX]	4.607	4.933	2.910	2.815
	F_{33}	F[OCrO]	1.306	1.050	1.102	1.219
	F_{44}	F[XCrX]	0.527	0.440	0.530	0.488
	F_{12}		0.392	0.569	0.258	[0.25]
	F_{13}		0.019	[0]	−0.014	[0.20]
	F_{23}		0.034	[0]	−0.043	[0.08]
A_2	F_{55}	F[OCrX]	0.717	0.607	0.590	0.610
B_1	F_{66}	F[CrX]	4.375	4.559	2.805	2.450
	F_{77}	F[OCrX]	0.819	0.734	0.708	0.694
	F_{67}		0.115	0.070	0.222	0.050
B_2	F_{88}	F[CrO]	7.016	7.129	6.680	6.764
	F_{99}	F[OCrX]	0.827	0.706	0.680	0.682
	F_{89}		−0.050	0.401	−0.031	0.157

[a] The prime (′) refer to pairs of internal coordinates with no common bond, and the double prime (″) refer to pairs of internal coordinates with a common CrX bond. [b] Force constants in brackets are assumed values. The B_1 and B_2 blocks are interchanged in refs 38 and 39. The standard notation for C_{2v} symmetry has been employed in the present work.

TABLE 7: Calculated (B3-LYP/LanL2DZ) and Experimental Molecular Geometry and Vibrational Wavenumbers for $[Cr_2O_7]^{2-}$, with (a) No Solvation and (b) in Aqueous Solution, and Experimental and Calculated Force Constants (mdyn Å^{-1})

Molecular Geometry

	calc			
	(a)	(b)	expt[42]	scale factor
r(CrO1) (Å)	1.772	1.813	1.782	1.00
r(CrO2) (Å)	1.626	1.613	1.610	0.90
r(CrO3) (Å)	1.625	1.616	1.610	0.90
θ(CrOCr) (Å)	175.2	133.8	123.9	0.95
θ(O1CrO2) (deg)	109.4	106.1	106.4	0.95
θ(O1CrO3) (deg)	109.7	109.6	109.9	0.95
θ(O2CrO3) (deg)	109.4	110.4	110.4	0.95
θ(O3CrO3′) (deg)	109.3	110.6	109.6	0.95

Vibrational Wavenumbers

		calc					
		(a)		(b)			
		unscaled	scaled	unscaled	scaled	expt[44]	potential energy distribution[a]
a_1	ν_1	996	945	1021	970	966	ν(CrO2) (68), ν(CrO3) (29)
	ν_2	958	910	979	930	908,902	ν(CrO2) (29), ν(CrO3) (69)
	ν_3	490	482	521	517	566,554	ν(CrO1) (68), δ(OCr═O) (23)
	ν_4	386	376	393	383	377	ω(CrO_2) (82)
	ν_5	330	322	372	363	329	δ(CrO_2) (88)
	ν_6	216	214	223	219	329	ν(CrO1) (29), δ(O−Cr═O) (68)
	ν_7	16	15	120	117	255	δ(CrOCr) (90)
a_2	ν_8	992	942	1016	965	925	ν(CrO3) (97)
	ν_9	378	368	380	370		ρ(CrO_2) (37), τ(CrO_2) (59)
	ν_{10}	218	213	228	223		ρ(CrO_2) (63), τ(CrO_2) (36)
	ν_{11}	11	11	53	52		τ(CrO_3) (99)
b_1	ν_{12}	997	947	1021	969	890, 885	ν(CrO3) (97)
	ν_{13}	385	375	390	380	390	τ(CrO_2) (86)
	ν_{14}	329	320	344	336	329	ρ(CrO_2) (88)
	ν_{15}	10	9	122	109		τ(CrO_3) (93)
b_2	ν_{16}	991	941	1019	968	958, 950	ν(CrO2) (66), ν(CrO3) (31)
	ν_{17}	940	924	956	907	938, 935	ν(CrO2) (32), ν(CrO3) (66)
	ν_{18}	907	875	786	785	764	ν(CrO1) (95)
	ν_{19}	386	376	384	374	390	δ(O−Cr═O) (22), δ(CrO_2) (54), ω(CrO_2) (23)
	ν_{20}	379	369	373	363	377	δ(CrO_2) (40), ω(CrO_2) (51)
	ν_{21}	220	214	222	222	370	δ(O−Cr═O) (69), ρ(CrO_2) (23)

Scaled Force Constants

	calc		
	(a)	(b)	expt
f[CrO2]	6.092	6.466	6.05
f[CrO3]	6.124	6.466	6.05
f[CrO1]	3.789	3.303	3.25
f[CrO2,CrO3]	0.376	0.422	0.58
f[CrO3,CrO3′]	0.376	0.422	0.58
f[CrO2,CrO2′]	0.063	0.031	0.08
f[CrO1,CrO2]	0.261	0.313	0.55
f[CrO1,CrO1′]	0.309	0.382	0.10
f[O1CrO2]	0.624	0.695	0.57
f[O1CrO3]	0.617	0.674	0.57
f[CrO1Cr]	0.013	0.650	0.17
f[CrO1,CrO1Cr]	0.025	0.317	0.00

[a] The potential energy distributions relate to the scaled force field for aqueous $[Cr_2O_7]^2$.

7, together with the vibrational wavenumbers calculated for the gas-phase near-linear geometry.

The gas-phase near-linear geometry gives symmetric and antisymmetric ν(Cr−O) vibrations that are too far apart, with the symmetric stretch much lower than the experimental value and the antisymmetric stretch too high. Also the Cr−O−Cr deformation is calculated to be at very low wavenumber (15 cm^{-1}). Even in the aqueous solution calculation, this vibration is predicted at 117 cm^{-1} which differs markedly from the reported position of 255 cm^{-1} for this vibration[44], and we therefore propose that the 255 cm^{-1} band be reassigned to the ν_6 mode, which is mainly O−Cr═O deformation.

Geometry optimization of $[Cr_3O_{10}]^{2-}$ with the CrOCr bond angles constrained to their experimental value (137.4°)[45] resulted in a structure with C_s symmetry. The optimization was then continued with the molecule constrained to have C_{2v} symmetry. This did not yield any imaginary vibrational wavenumbers and provided a satisfactory fit to the experimental vibrational spectrum (Table 8). Aqueous solution calculations were not attempted for $[Cr_3O_{10}]^{2-}$ because of its much larger size.

Relationship between CrO Stretching Force Constant and Bond Distance. From the structural and spectroscopic data, we have derived a relationship between the CrO bond distance and principal stretching force constants f[CrO]. There have been

TABLE 8: Calculated (B3-LYP/LanL2DZ) and Experimental Molecular Geometry and Vibrational Wavenumbers for $[Cr_3O_{10}]^{2-}$, with (a) Full Geometry Optimization and (b) Cr1O1Cr2 Angle Constrained to 137.4°, and Calculated Force Constants (mdyn Å^{-1}) (Constrained Geometry)

Molecular Geometry

	calc			
	(a)	(b)	expt[45]	scale factor
r(Cr1O1) (Å)	1.828	1.825	1.811	1.00
r(Cr2O1) (Å)	1.714	1.724	1.717	1.00
r(Cr1O2) (Å)	1.615	1.613	1.602	0.90
r(Cr1O3) (Å)	1.614	1.618	1.602	0.90
r(Cr2O4) (Å)	1.599	1.592	1.577	0.90
θ(Cr1O1Cr3) (deg)	154.3	137.4	137.4	0.95
θ(O1Cr1O2) (deg)	108.0	107.4	105.9	0.95
θ(O1Cr1O3) (deg)	109.2	109.2	109.4	0.95
θ(O2Cr1O3) (deg)	110.3	110.6	110.0	0.95
θ(O3Cr1O3′) (deg)	109.9	109.7	110.0	0.95
θ(O1Cr2O1′) (deg)	110.0	108.1	107.9	0.95
θ(O1Cr2O4) (deg)	109.6	110.2	110.1	0.95
θ(O4Cr2O4′) (deg)	108.4	108.7	108.6	0.95

Vibrational Wavenumbers

		calc					
		(a)		(b)			
		unscaled	scaled	unscaled	scaled	expt[45]	potential energy distribution
a_1	ν_1	1023	972	1027	976	976	ν(Cr1O3) (15), ν(Cr2O4) (76)
	ν_2	1016	965	1011	960	947	ν(Cr1O2) (52), ν(Cr1O3) (28), ν(Cr2O4) (17)
	ν_3	965	934	960	911		ν(Cr1O2) (42), ν(Cr1O3) (54)
	ν_4	934	915	884	883	887	ν(Cr1O1) (31), ν(Cr2O1) (66)
	ν_5	490	482	535	529		ν(Cr1O1) (31), ν(Cr2O1) (66), δ(O1Cr2O1′) (19)
	ν_6	394	384	394	385		δ(O4Cr2O4′) (79)
	ν_7	383	373	383	373	372	δ(O3Cr1O3′) (54), ρ(O3Cr1O3′) (40)
	ν_8	362	353	374	365		δ(O3Cr1O3′) (36), ρ(O3Cr1O3′) (34), δ(O1Cr2O1′) (13), δ(O4Cr2O4′) (12)
	ν_9	212	207	210	205		δ(O2Cr1O1) (82)
	ν_{10}	132	130	126	124		ν(Cr1O1) (21), δ(Cr1O1Cr2) (13), ρ(O3Cr1O3′) (10), δ(O1Cr2O1′) (46)
	ν_{11}	31	31	48	47		δ(Cr1O1Cr2) (81), δ(O1Cr2O1′) (19)
a_2	ν_{12}	1019	968	1019	967		ν(Cr1O3) (97)
	ν_{13}	379	369	379	369		ω(O3Cr1O3′) (30), τ(Cr1O3) (65)
	ν_{14}	334	326	338	329		ω(O3Cr1O3′) (30), τ(Cr2O4) (61)
	ν_{15}	208	203	208	203		ω(O3Cr1O3′) (38), τ(Cr1O3) (25), τ(Cr2O4) (36)
	ν_{16}	43	42	69	67		$\tau(CrO_3)$ (41), τ(O1Cr2) (53)
	ν_{17}	11	11	34	33		$\tau(CrO_3)$ (59), τ(O1Cr2) (41)
b_1	ν_{18}	1043	990	1052	998	999	ν(Cr2O4) (93)
	ν_{19}	1020	968	1018	967		ν(Cr1O3) (93)
	ν_{20}	381	371	381	371		ω(O3Cr1O3′) (67), ω(O4Cr2O4′) (10), τ(Cr1O2) (20)
	ν_{21}	354	345	358	348		ω(O4Cr2O4′) (60), τ(Cr1O3) (35)
	ν_{22}	216	210	215	210		ω(O3Cr1O3′) (30), ω(O4Cr2O4′) (24), τ(Cr1O3) (45)
	ν_{23}	29	28	52	51		$\tau(CrO_3)$ (76), τ(O1Cr2) (19)
	ν_{24}	14	14	15	15		$\tau(CrO_3)$ (19), τ(O1Cr2) (80)
b_2	ν_{25}	1018	967	1012	961	967	ν(Cr1O2) (50), ν(Cr1O3) (46)
	ν_{26}	972	934	962	918	916	ν(Cr1O2) (41), ν(Cr1O3) (42), ν(Cr2O1) (14)
	ν_{27}	888	876	850	845	859	ν(Cr1O3) (10), ν(Cr1O1) (19), ν(Cr2O1) (62)
	ν_{28}	494	489	513	510	515	ν(Cr1O1) (63), ν(Cr2O1) (16)
	ν_{29}	389	379	392	382		ρ(O4Cr2O4′) (35), ρ(O3Cr1O3′) (21), δ(O3Cr1O3′) (29)
	ν_{30}	372	362	373	364		ρ(O4Cr2O4′) (32), δ(O3Cr1O3′) (53)
	ν_{31}	317	311	335	328		ν(Cr1O1) (14), δ(O3Cr1O3′) (12), ρ(O3Cr1O3′) (60)
	ν_{32}	203	199	204	199		ρ(O4Cr2O4′) (17), δ(O2Cr1O1) (69)
	ν_{33}	70	68	89	87		δ(Cr1O1Cr2) (89)

Scaled Force Constants

f[Cr1O2]	6.252	*f*[Cr2O1,Cr2O1′]	0.283
f[Cr1O3]	6.446	*f*[O1Cr1O2]	0.616
f[Cr2O4]	6.895	*f*[O1Cr1O3]	0.594
f[Cr1O1]	2.869	*f*[Cr1O1Cr2]	0.298
f[Cr2O1]	4.687	*f*[O2Cr2O1′]	0.708
f[Cr1O2,Cr1O3]	0.393	*f*[O2Cr1O3]	0.883
f[Cr1O3,Cr1O3′]	0.390	*f*[O2Cr1O3′]	0.905
f[Cr2O4,Cr2O4′]	0.383	*f*[O1Cr2O4]	0.706
f[Cr1O1,Cr2O1]	0.406	*f*[O4Cr2O4′]	0.994

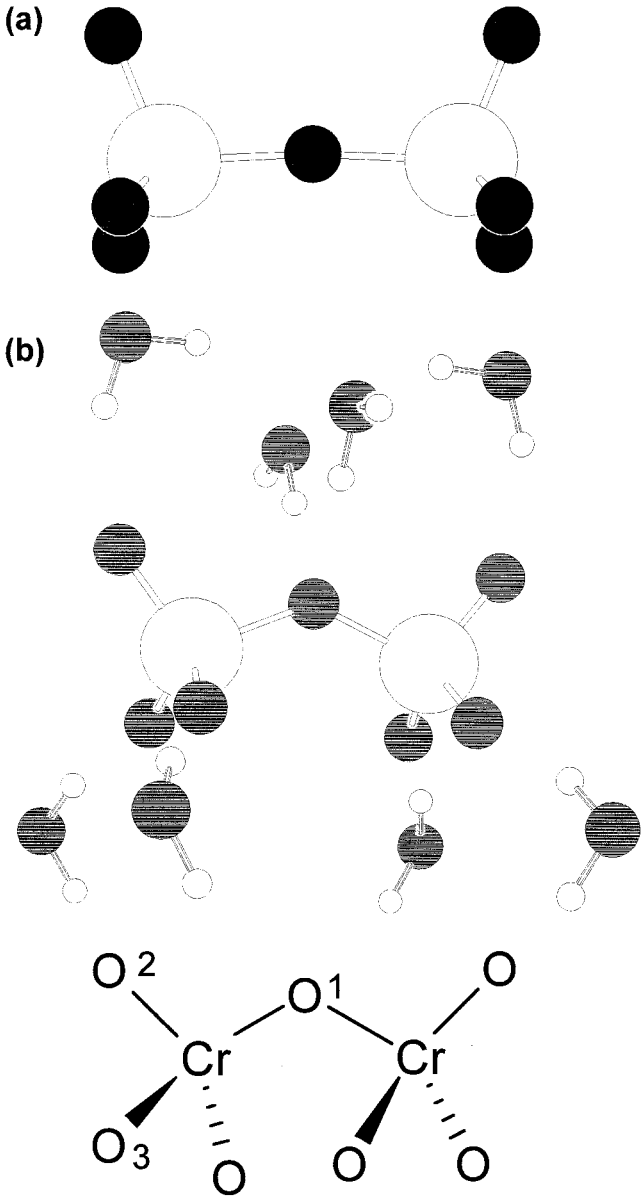

Figure 4. Calculated molecular geometry for $[Cr_2O_7]^{2-}$ with (a) full optimization and (b) CrOCr angle constrained to 123E, and atom numbering scheme.

many attempts to relate bond distances to stretching force constants, of which the most popular is Badger's rule:[46]

$$f_r = \frac{C}{(r-d)^3} \tag{1}$$

The best fit to this equation for calculated force constants and experimentally determined bond distances, shown in Figure 6a, was obtained with $C = 2.25 \pm 0.05$ mdyn Å^2 and $d = 0.9 \pm 0.05$ Å. The most significant deviation from the plot is for the halochromates $[CrO_3X]^-$, which may, in part, be due to the poor structural data for the $[CrO_3X]^-$ anions. The plot suggests that the CrO distance should be shorter in $[CrO_3F]^-$ and longer in $[CrO_3Cl]^-$; omitting these two points, the R^2 value for the fit is 0.974. We believe it is possible also that the halogen atoms may exert an electronic effect that is reflected in the force constants but not in the bond distances.

Although Badger's Rule has been employed over many decades there appears to be no sound theoretical justification and we have sought to fit the data to a simpler function. In fact

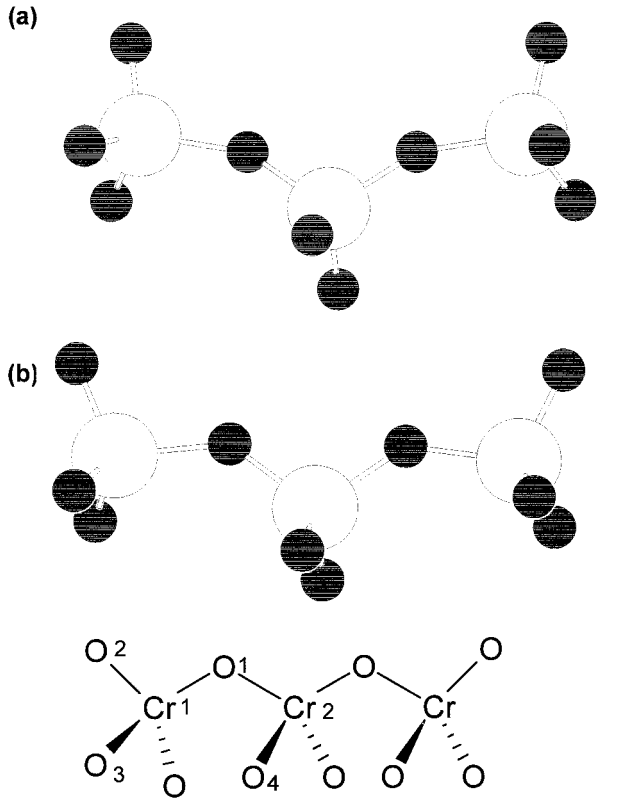

Figure 5. Calculated molecular geometry for $[Cr_3O_{10}]^{2-}$ with (a) full optimization and (b) CrOCr angle constrained to 137.4E, and atom numbering scheme.

it is possible to obtain an excellent fit to the data with a simple linear function of the type

$$f_r = a_r + b \tag{2}$$

Using this function, the relationship between the scaled force constants to the experimental bond distances gives a best fit of $a = -16.54 \pm 1.24$ mdyn Å^{-2} and $b = 32.94 \pm 2.03$ mdyn Å^{-1}, with $R^2 = 0.937$, shown in Figure 6b. Fitting the scaled force constants to calculated bond distances, shown in Figure 6c, gives the parameters $a = -16.71 \pm 0.58$ mdyn Å^{-2} and $b = 33.41 \pm 0.96$ mdyn Å^{-1}, $R^2 = 0.986$. Again, it is seen that the halochromate species give a poor fit in the first instance, reflecting the dubious nature of their experimentally determined bond distances. When comparing scaled force constants with calculated bond distances, the halochromates lie close to the linear fit.

In a recent paper, Weckhuysen and Wachs[47] have attempted to derive a relationship between CrO bond distances, stretching vibrations, and bond valences in a range of chromium(VI) oxo-anions and supported chromium(VI) oxide catalysts. We consider this approach to be unjustifiable on the grounds that the vibrational wavenumber is a function of both force constant and molecular geometry. It is therefore more realistic to consider the relationship between force constant and bond distance and to relate the CrO bond valence to the CrO stretching force constant. Brown and Wu[48] suggest that bond distance and bond valence s, are related by the following equation:

$$s(\mathrm{CrO}) = \left[\frac{r(\mathrm{CrO})}{1.787}\right]^{-5.0} \tag{3}$$

where 1.787 Å is the bond distance attributed to a Cr−O bond of unit bond order. Combining eq 3 with eqs 1 or 2, we obtain

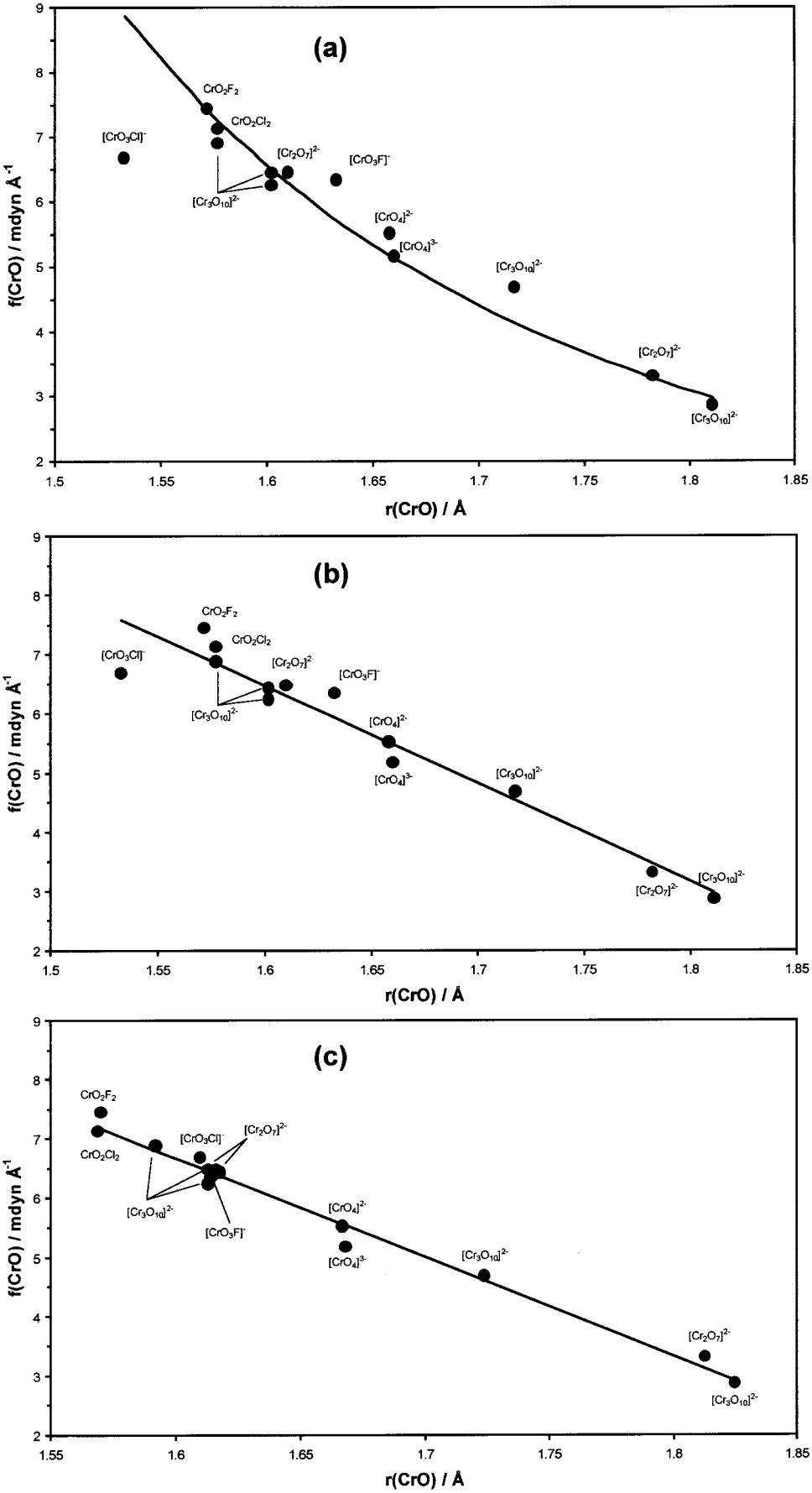

Figure 6. Plot of CrO bond distance versus principal CrO stretching force constant: (a) scaled force constants versus experimental bond distances, fitted using Badger's rule, (b) linear fit of scaled force constants versus experimental bond distances, and (c) linear fit of scaled force constants versus calculated bond distances. The points (●) are the data, and the lines are the least squares best fits.

TABLE 9: CrO Bond Valences Determined from Force Constants Using (a) Badger's Rule Plot, (b) Linear Plot with Experimental Bond Distances, and (c) Linear Plot with calculated bond distances

molecule (bond)	*f*[CrO] (mdyn Å^{-1})	s(CrO) (a)	(b)	(c)
$[Cr_3O_{10}]^{2-}$ (Cr1O1)	2.869	0.907	0.934	1.038
$[Cr_2O_7]^{2-}$ (CrO1)	3.303	1.020	1.002	1.116
$[Cr_3O_{10}]^{2-}$ (Cr2O1)	4.687	1.350	1.259	1.417
$[CrO_4]^{3-}$	5.172	1.456	1.367	1.545
$[CrO_4]^{2-}$	5.530	1.532	1.454	1.649
$[Cr_3O_{10}]^{2-}$ (Cr1O2)	6.252	1.678	1.652	1.884
$[CrO_3F]^{-}$	6.345	1.696	1.679	1.917
$[Cr_3O_{10}]^{2-}$ (Cr1O3)	6.446	1.716	1.710	1.954
$[Cr_2O_7]^{2-}$ (CrO2)	6.466	1.720	1.716	1.961
$[Cr_2O_7]^{2-}$ (CrO3)	6.466	1.720	1.716	1.961
$[CrO_3Cl]^{-}$	6.684	1.762	1.785	2.044
$[Cr_3O_{10}]^{2-}$ (Cr2O4)	6.895	1.802	1.854	2.123
CrO_2Cl_2	7.122	1.845	1.934	2.223
CrO_2F_2	7.443	1.904	2.052	2.366

eq 4 for the Badger's Rule fit and eq 5 for the linear fit.

$$s(\mathrm{CrO}) = \left[\frac{f(\mathrm{CrO})^{-0.333} + 0.687}{1.364}\right]^{-5.0} \quad (4)$$

$$s(\mathrm{CrO}) = \left[\frac{f(\mathrm{CrO}) - b}{1.787a}\right]^{-5.0} \quad (5)$$

Using these equations, we have determined bond valences for all of the species studied, and these are listed in Table 9. The s(CrO) values obtained using Badger's rule and the linear fit of scaled force constants versus experimental bond distances are comparable. The linear fit of scaled force constants versus calculated bond distances gives significantly larger s(CrO) values, and these are regarded as less satisfactory. We also attempted to derive a relationship between OCrO bond angles and the principal deformation force constants f[OCrO]. Although there is a general trend for *f*[OCrO] to decrease with increasing bond angle, the data points are widely scattered and no satisfactory relationship could be established.

Conclusion

In this paper, we have established that calculations of the vibrational spectra of chromates and related species give an excellent fit to the experimental data using the B3-LYP method in conjunction with the LanL2DZ basis set, with only slight scaling. Larger basis sets such as 6-31G and 6-311G gave less satisfactory results, even with the inclusion of several polarization and diffuse functions, and such calculations required much greater computational resources. Our findings somewhat contradict those of Wong,[49,50] who reported calculations of several small inorganic molecules using the same basis sets in conjunction with HF-SCF, B3-LYP, and other density functional methods. They concluded that the agreement between theory and experiment was better for 6-311G(d) than LanL2DZ calculations, although only marginally so.

Calculations of optimized geometries at the B3-LYP/LanL2DZ level give an excellent fit to the experimental geometries with two exceptions. These are the dichromate and trichromate species, for which the calculations suggest near-linear CrOCr bond angles. For this reason, the geometries of these anions were recalculated with those angles constrained to their experimentally determined values.

The calculation of vibrational spectra has enabled complete sets of force constants and potential energy distributions to be derived. In two cases, a partial reassignment of the experimental spectra has been indicated by the calculations. A linear relationship was established between the principal stretching force constants *f*[CrO] and CrO bond distances. From the results of this study, we have embarked on an investigation of the chromate species on the surfaces of supported chromium(VI) oxide catalysts, and this will be reported in a future paper.

References and Notes

(1) Durig, J. R.; Guirgis, G. A.; Kim, Y. H.; Yan, W. H.; Qtait, M. A. *J. Mol. Struct.* **1996**, *382*, 111.
(2) Guirgis, G. A.; Shens, Z. N.; Qtait, M. A.; Durig, J. R. *J. Mol. Struct.* **1997**, *403*, 57.
(3) Alvarez, R. M. S.; Cutin, E. H.; Mack, H. G.; Della Vedova, C. O. *Chem. Ber.* **1997**, *130*, 1141.
(4) Bailey, L. E.; Navarro, R.; Hernanz, A. *Biospectroscopy* **1997**, *3*, 47.
(5) Parr, R. G.; Yang, W. *Density Functional Theory of Atoms and Molecules*; Oxford University Press: Oxford, 1989.
(6) Becke, A. D. *J. Chem. Phys.* **1993**, *98*, 5648.
(7) Lee, C.; Yang W.; Parr, R. G. *Phys. Rev. B* **1988**, *37*, 785.
(8) Choi, C. H.; Kertesz, C. *J. Phys. Chem.* **1996**, *100*, 16530.
(9) Gallinella, E.; Cadioli, B. *Vib. Spectrosc.* **1997**, *13*, 163.
(10) Bauschlicher, C. W.; Langhoff, S. R.; Sandford, S. A.; Hudgins, D. M. *J. Phys. Chem. A* **1997**, *101*, 2414.
(11) Ma, B.; Lii, J. J.; Schaefer, H. F.; Allinger, N. L. *J. Phys. Chem.* **1996**, *100*, 8763.
(12) Bell, S. *Vibrational Spectra and Structure*; Durig, J. R., Ed.; Vol. 24; Elsevier: Amsterdam, 2000; p 253.
(13) Hardcastle, F. D.; Wachs, I. E. *J. Mol. Catal.* **1988**, *46*, 173.
(14) Weckhuysen, B. M.; Schoonheydt, R. A.; Jehng, J. M..; Wachs, I. E.; Cho, S. J.; Ryoo, R.; Kijlstra, S.; Poels, E. *J. Chem. Soc., Faraday Trans.* **1995**, *91*, 3245.
(15) Weckhuysen, B. M.; Wachs, I. E. *J. Phys. Chem.* **1992**, *96*, 5008.
(16) Vuurman, M. A.; Wachs, I. E. *J. Phys. Chem. B* **1997**, *101*, 2793.
(17) Vuurman, M. A.; Wachs, I. E.; Stufkens, D. J.; Oskam, A. *J. Mol. Catal.* **1993**, *80*, 209.
(18) Vuurman, M. A.; Hardcastle, F. D.; Wachs, I. E. *J. Mol. Catal.* **1993**, *84*, 193.
(19) Jehng, J. M.; Turek, A. M.; Wachs, I. E. *Appl. Catal. A* **1992**, *83*, 179.
(20) Kim, D. S.; Tatibouet, J. M.; Wachs, I. E. *J. Catal.* **1992**, *136*, 209.
(21) Kim, D. S.; Wachs, I. E. *J. Catal.* **1993**, *142*, 209.
(22) Jehng, J. M.; Wachs, I. E.; Weckhuysen, B. M.; Schoonheydt, R. A. *J. Chem. Soc., Faraday Trans.* **1995**, *91*, 953.
(23) *Gaussian 98, Revision A.5*, Frisch, M. J.; Trucks, G. W.; Schlegel, H. B.; Scuseria, G. E.; Robb, M. A.; Cheeseman, J. R.; Zakrzewski, V. G.; Montgomery, J. A. Jr.; Stratmann, R. E.; Burant, J. C.; Dapprich, S.; Millam, J. M.; Daniels, A. D.; Kudin, K. N.; Strain, M. C.; Farkas, O.; Tomasi, J.; Barone, V.; Cossi, M.; Cammi, R.; Mennucci, B.; Pomelli, C.; Adamo, C.; Clifford, S.; Ochterski, J.; Petersson, G. A.; Ayala, P. Y.; Cui, Q.; Morokuma, K.; Malick, D. K.; Rabuck, A. D.; Raghavachari, K.; Foresman, J. B.; Cioslowski, J.; Ortiz, J. V.; Stefanov, B. B.; Liu, G.; Liashenko, A.; Piskorz, P.; Komaromi, I.; Gomperts, R.; Martin, R. L.; Fox, D. J.; Keith, T.; Al_Laham, M. A.; Peng, C. Y.; Nanayakkara, A.; Gonzalez, C.; Challacombe, M.; Gill, P. M. W.; Johnson, B.; Chen, W.; Wong, M. W.; Andres, J. L.; Gonzalez, C.; Head_Gordon, M.; Replogle, E. S.; Pople, J. A. Gaussian, Inc.; Pittsburgh, PA., 1998.
(24) Hay, P. J.; Wadt, W. R. *J. Chem. Phys.* **1985**, *82*, 270, 284 and 299.
(25) Schachtschneider, J. A. *Vibrational Analysis of Polyatomic Molecules*, Parts V and VI, Technical Report Nos. 231 and 57, Shell Development Co.: Houston, TX, 1964 and 1965.
(26) Weber, G.; Range, K. J. *Z. Naturfor. B* **1996**, *51*, 751.
(27) Kiefer, W.; Bernstein, H. J. *Mol. Phys.* **1972**, *23*, 835.
(28) Deeth, R. J.; Sheen, P. D. *J. Chem. Soc., Faraday Trans.* **1994**, *90*, 3237.
(29) Stückl, A. C.; Daul, C. A.; Güdel, H. U. *J. Chem. Phys.* **1997**, *107*, 4606.
(30) Weinstock, N.; Schulze, H.; Müller, A. *J. Chem. Phys.* **1973**, *59*, 5063.
(31) Bassi, D.; Sala, O. *Spectrochim. Acta* **1958**, *12*, 403.
(32) Gonzalez-Vilchez, F.; Griffith, W. P. *J. Chem. Soc., Dalton Trans.* **1972**, 1416.
(33) Wilhelmi, K. A.; Jonsson, O. *Acta Chem. Scand.* **1965**, *19*, 177.
(34) Roegner, P.; Range, K. J. *Z. Naturfor. B* **1995**, *50*, 1412.
(35) Helmholz, L.; Foster, W. R. *J. Am. Chem. Soc.* **1950**, *72*, 4971.
(36) Stammreich, H.; Sala, O.; Kawai, K. *Spectrochim. Acta* **1963**, *19*, 593.

(37) Stammreich, H.; Sala, O.; Bassi, D. *Spectrochim. Acta* **1961**, *17*, 226.
(38) French, R. J.; Hedberg, L.; Hedberg, K.; Gard, G. L.; Johnson, B. M. *Inorg. Chem.* **1982**, *22*, 892.
(39) Marsden, C. J.; Hedberg, L.; Hedberg, K. *Inorg. Chem.* **1982**, *21*, 1115.
(40) Brown, S. D.; Gard, G. L.; Loehr, T. M. *J. Chem. Phys.* **1976**, *64*, 1219.
(41) Stammreich, H.; Kawai, K.; Tavares, Y. *Spectrochim. Acta* **1959**, *15*, 438.
(42) Brunton, G. *Mater. Res. Bull.* **1973**, *8*, 271.
(43) Wong, M. W.; Wiberg, K. B.; Frisch, M. J. *J. Chem. Phys.* **1991**, *95*, 8991.
(44) Brown, R. G.; Ross, S. D. *Spectrochim. Acta* **1972**, *28A*, 1263.
(45) Pressprich, M. R.; Willet, R. D.; Poshusta, R. D.; Saunders: S. C.; Davies, H. B.; Gard, G. L. *Inorg. Chem.* **1988**, *27*, 260.
(46) Badger, R. M. *J. Chem. Phys.* **1934**, *2*, 128; **1935**, *3*, 710.
(47) Weckhuysen, B. M.; Wachs, I. E. *J. Chem. Soc., Faraday Trans.* **1996**, *92*, 1969.
(48) Brown, I. D.; Wu, K. K. *Acta Crystallogr.* **1976**, *32B*, 1947.
(49) Wong, M. W. *Chem. Phys. Lett.* **1996**, *256*, 391.
(50) Bytheway, I.; Wong, M. W. *Chem. Phys. Lett.* **1998**, *282*, 219.